micrographs (Fig. 4) of the same region, which clearly show that the regions on either side of the boundary are purely (001) or (012) oriented.

A further examination of the boundaries revealed that in most of the cases the two orientations had the [110] reciprocal lattice direction common except for some rare observations such as the one mentioned above. It may be mentioned that irradiation of the film with the electron beam resulted in the re-orientation of the grains to have a common [110] reciprocal lattice direction. Similar results were observed when the films were aged in vacuum for a couple of days.

The appearance of (012) and (011) orientations in continuous bismuth films seems to be the result of the growth rates of the nuclei rather than their initial orientation. The (001) and (012) oriented grains usually have a common [110] reciprocal lattice direction or re-orient to have the common direction during observations under electron beam irradiation. Ageing of the films has a similar effect on the re-orientation of the films.

Acknowledgements

The authors wish to thank Dr T. C. Patel for his help with the electron microscopy work and also the Council of Scientific and Industrial Research, Government of India for the financial assistance to G.K.S.

References

1. YU. F. KOMNIK and V. V. PILIPENKO, *Sov. Phys. Crystallogr.* **16** (1971) 352.
2. V. M. KOSEVICH, L. S. PALSTNIK, S. N. GRIGOROV and YU. V. ZOLOTNITSKII, *Sov. Phys. Solid State* **11** (1970) 2547.
3. A. A. ZAVYALOVA and R. M. IMANOV, *Sov. Phys. Crystallogr.* **14** (1969) 305.
4. A. I. FEDERENKI, L. S. PALATNIK and V. M. KOSEVICH, *Sov. Phys. Solid State* **9** (1968) 2238.

Received 6 October
and accepted 27 October 1976

A. R. PATEL
G. K. SHIVAKUMAR
Department of Physics, Sardar Patel University,
Vallabh Vidyanagar, 388120,
Gujarat State,
India

Direct evidence for a brucite precipitate in a melt-grown MgO crystal

Since the studies of the infra-red absorption characteristics of MgO crystals by Kirklin *et al.* in 1965 [1] suggested that an absorption band found at 3700 cm^{-1} might be due to brucite ($Mg(OH)_2$) precipitates, other workers have accumulated further indirect evidence for the existence of such precipitates. Glass and Searle [2] also found a strong absorption peak at 3700 cm^{-1} which they attributed to the presence of brucite precipitates, whilst Sibley *et al.* [3] provided further confirmation by luminescence measurements. Briggs [4] reported the observation of a strong absorption at 3698 cm^{-1} in subsurface regions of MgO crystals containing relatively high levels of hydroxyl impurity. He also assumed that this absorption was due to brucite precipitates, on the basis of earlier work on $Mg(OH)_2$ crystals by Cabannes-Ott [5], who established the fundamental OH stretching frequency in $Mg(OH)_2$ at 3700 ± 4 cm^{-1}, and Benesi [6], who found the brucite OH stretching frequency at 3698 ± 2 cm^{-1}.

Buessem and Köberich [7] found that the transformation brucite to periclase (MgO) was crystallographically ordered, and that the brucite formed on rehydration of the periclase had the same orientation relations with the periclase as had the original brucite. These orientation relations for the transformation were examined in detail by Garrido [8, 9], who established that MgO crystallites formed from $Mg(OH)_2$ had two possible orientations in which the zone axes, with respect to those of the brucite, were as shown in Table I. That is, in the MgO resulting from thermal decomposition of brucite, the close-packed planes of oxygen ions lie parallel to the close-packed

TABLE I Orientation relations of periclase and brucite

Orientation	Periclase crystal direction	Brucite crystal direction
I	[110]	$[10\bar{1}0]$
	[111]	[0001]
	[100]	$[10\bar{1}1]$
II	[110]	$[10\bar{1}0]$
	[111]	[0001]
	[100]	$[1\bar{1}01]$

planes of hydroxyl ions in the brucite, and the *c*- and *a*-directions of the brucite become the [1 1 1] and [1 1 0] directions of the MgO. These relationships were later confirmed by Ball and Taylor [10], Goodman [11] and Brindley [12]. On the basis of this evidence there is good reason to believe that, if brucite precipitates exist in MgO crystals, their topological relationships to their matrix should be predictable. For example, if a brucite precipitate could be observed in an electron microscope specimen cleaved parallel to a {1 0 0} plane, it should have the $[1\,0\,\bar{1}\,1]$ or the equivalent $[1\,\bar{1}\,0\,1]$ zone axis, and should readily be identifiable by its electron diffraction pattern. The present work describes the results of an electron microscope search for $Mg(OH)_2$ precipitates in melt-grown MgO crystals.

10 mm cube samples of Spicer MgO crystal with {1 0 0} faces were extracted from crude, melt-grown lumps by cleavage, using a hammer and hardened steel blade. A pendulum cleaving machine was then used to obtain 0.5 mm thick slices by successive splitting operations, each time cleaving into halves the slices obtained. Still thinner slices were cleaved by holding the 0.5 mm slices and a new single-edged razor blade between finger and thumb and tapping the blade sharply with a hammer. The {1 0 0} slices obtained were placed in a perforated polytetrafluorethlyene holder and chemically thinned by immersion in dilute orthophosphoric acid at 120° C. Continuous agitation in the acid, and frequent transfer to clean, boiling water was found to be necessary to avoid contamination of the specimen surfaces. When the area of a specimen had been reduced to 2 to 3 mm^2 it contained electron-transparent regions and was suitable for transmission electron microscopy. It was then mounted on a copper grid smeared with polybutane and stored in a vacuum desiccator until it could be examined, usually within a few hours.

Electron microscope examination was carried out in a J.E.M.7 microscope. Many crystalline precipitates were found and photographed, and their selected-area electron diffraction patterns recorded. In most cases the patterns could not be identified, but one precipitate gave the pattern shown in Fig. 1a which, as shown in Table II and III, has parameters close to those expected from a brucite precipitate with the anticipated orien-

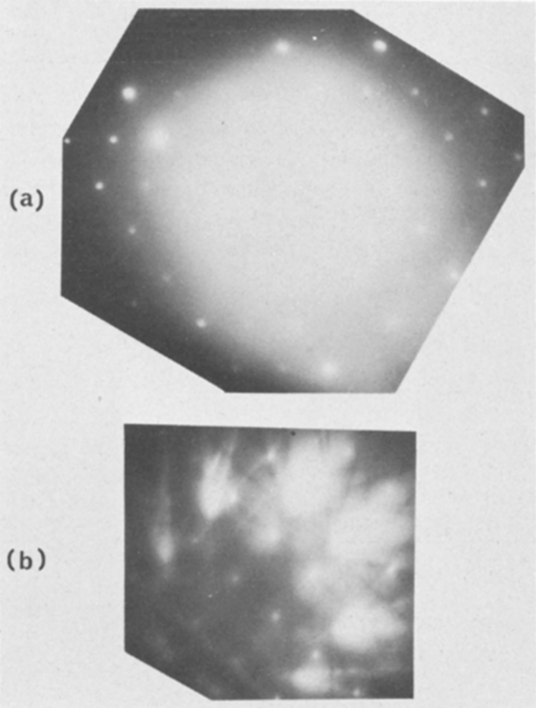

Figure 1 (a) Selected-area diffraction pattern from a precipitate. (b) Matrix diffraction pattern from a point close to the precipitate.

TABLE II Computed parameters for the brucite $[1\,0\,\bar{1}\,1]$ reciprocal lattice net

Lattice plane	R^* (mm)	*d*-spacing (Å)
$(1\,\bar{1}\,0\,\bar{1})$	6.25	2.36
$(\bar{1}\,\bar{1}\,0\,\bar{1})$	6.25	2.36
$(0\,\bar{1}\,1\,1)$	6.25	2.36
$(0\,1\,\bar{1}\,\bar{1})$	6.25	2.36
$(\bar{1}\,0\,1\,2)$	8.24	1.79
$(1\,0\,\bar{1}\,\bar{2})$	8.24	1.79
$(\bar{1}\,2\,\bar{1}\,0)$	9.40	1.57
$(1\,\bar{2}\,1\,0)$	9.40	1.57

TABLE III Experimental parameters for a precipitate reciprocal lattice net

Lattice plane	R^* (mm)	*d*-spacing (Å)
$(1\,\bar{1}\,0\,\bar{1})$	6.3	2.34
$(\bar{1}\,1\,0\,\bar{1})$	6.3	2.34
$(0\,\bar{1}\,1\,1)$	6.3	2.34
$(0\,1\,\bar{1}\,\bar{1})$	6.3	2.34
$(\bar{1}\,0\,1\,2)$	7.8	1.89
$(1\,0\,\bar{1}\,\bar{2})$	7.8	1.89
$(\bar{1}\,2\,\bar{1}\,0)$	10.0	1.47
$(1\,\bar{2}\,1\,0)$	10.0	1.47

tation relationships to the MgO matrix. The precipitate disappeared during the diffraction exposure, leaving a residue indistinguishable from the surrounding matrix. Included in Fig. 1 is a matrix diffraction pattern obtained from a nearby area, which was used for orientation of the precipitate pattern. Twenty such matrix patterns were used to obtain an average value of 1.474 for the microscope's camera constant, from which the R^* and hence d-spacing data in Table III were computed. R^* is the distance between the origin of the diffraction pattern and the appropriate diffraction spot appearing on a photographic plate, and d is calculated from $R^* d = \lambda L$, where λL is the camera constant.

Taking into account the inherent inaccuracies involved in the recording and measurement of selected-area electron diffraction patterns, the resemblance of the theoretical and experimental lattice parameters is good. The small differences may partially be attributed to tilting of the specimen with respect to the electron beam. No useful matrix reflections appear in the pattern of Fig. 1a but a magnesium oxide pattern obtained from a nearby area of the same specimen is shown in Fig. 1b. Distortion of this pattern shows the specimen to be tilted, and the amount of tilt may be calculated from the displacement of the Kikuchi lines observed. There is a rotation of 2θ about [2 0 0] and $\theta/2$ about [0 2 0], where θ is the Bragg angle for the MgO {0 0 2} planes,

$$2\lambda = 2d \sin\theta$$

and

$$\sin\theta = \frac{\lambda}{d_{\{0\,0\,2\}}} = \frac{0.037}{2.10} = 0.0176.$$

The displacement of the specimen from the electron beam direction is, therefore, 2° about [2 0 0] and 0.5° about [0 2 0].

Disappearance of the precipitate during the recording of its diffraction pattern is consistent with its being brucite which was found by previous workers [10, 11, 13] to begin to decompose to MgO ~ 250° C, a temperature which may be reached in the conditions of the electron microscope under beam heating [11]. The presence of brucite in melt-grown MgO crystals is at first sight puzzling since, during melting, the matrix material reaches a temperature $> 2800°$ C, the melting point of MgO. It argues for a high solubility of hydroxyl ions in molten MgO and in high temperature solid MgO, and agglomeration and ordering of these to form brucite as the MgO cools. Malinowski *et al.* [14] showed by infra-red absorption techniques that MgO powders after heating to 1300° C still contained OH^- groups, and according to Nielson and Leipold [15] dense MgO, hot-pressed from fine powders, still contained 100 to 1000 ppm hydroxyl ions after reheating to 2200° C and high vacuum bake-out. At very high temperatures Stotz and Wagner [16] showed that in NiO and CoO, which are isomorphous with MgO, for a given water vapour partial pressure, there should be an increase in OH^- content due to true equilibrium solubility. If, during cooling, the equilibrium concentration of OH^- in MgO cannot be adjusted by its diffusion to the surface, as is probable in large crystals, agglomeration of the OH^- in some form may be an alternative means of reducing its solubility. Meyer and Yang [17] have examined the equilibrium relationships for the reaction

$$Mg(OH)_2 = MgO + H_2O$$

as a function of pressure and temperature. Extrapolation of their curve suggests that, under a pressure of 3500 MN m^{-2} brucite could be stable up to the melting point of MgO. The much lower temperatures at which the brucite probably precipitates would require much lower pressures for its stability; pressures well within the ability of the matrix to contain them.

Acknowledgement

My thanks are due to Dr D. H. Bowen who drew my attention to the topological relationships between MgO and brucite, and in particular to the work of Garrido.

References

1. P. W. KIRKLIN, P. AUZINS and J. E. WERTZ, *J. Phys. Chem. Solids* **26** (1965) 1067.
2. A. M. GLASS and T. M. SEARLE, *J. Chem. Phys.* **46** (1967) 2092.
3. W. A. SIBLEY, C. M. NELSON and Y. CHEN, *ibid* **48** (1968) 4582.
4. A. BRIGGS, *J. Mater. Sci.* **10** (1975) 729.
5. C. CABANNES-OTT, *Compt. Rend. Acad. Sci.* **203** (1936) 94.
6. H. A. BENESI, *J. Chem. Phys.* **30** (1959) 852.
7. W. BUESSEM and F. KÖBERICH, *Z. Phys. Chem.* **B17** (1932) 310.

8. J. GARRIDO, *Ion. Rev. Espan. Quim. Aplic.* **11** (1951) 206.
9. *Idem, ibid* **11** (1951) 453.
10. M. C. BALL and H. F. W. TAYLOR, *Min. Mag.* **32** (1961) 754.
11. J. F. GOODMAN, *Proc. Roy. Soc. A* **247** (1958) 346.
12. G. W. BRINDLEY, *Prog. Ceram. Sci.* 3 (1963) 7.
13. P. J. ANDERSON, R. F. MORLOCK and J. F. OLIVER, *Trans. Faraday Soc.* **61** (1965) 2754.
14. S. MALINOWSKI, S. SZCZEPANSKA and J. SLOCZYNSKI, *J. Catalysis* 7 (1967) 67.
15. T. H. NIELSON and M. H. LEIPOLD, *J. Amer. Ceram. Soc.* 49 (1966) 626.
16. S. STOTZ and C. WAGNER, *Ber. Bunsenges. Phys. Chem.* 70 (1966) 781.
17. J. W. MEYER and J. YANG, *Amer. J. Sci.* **260** (1962) 707.

Received 11 October
and accepted 28 October 1976

A. BRIGGS
Materials Development Division,
Building 552,
AERE, Harwell,
UK

Formation and structure of striations on the fracture surface of glassy polystyrene

In glassy amorphous polymers the fracture surface produced by tensile or bend loading often consists of a smooth mirror zone at the onset of fracture and of a rough striation zone in the region of rapid crack propagation (Fig. 1) [1]. Kusy *et al.* recently investigated these characteristic markings under different aspects of fracture in PMMA [2, 3]. Their observations agree with many of the results which we have obtained on PS (PS 168 N, BASF) [4]. The purpose of this work is to describe further details of the band structure. An energy criterion will be used to explain the formation of the bands, and together with the crack propagation model established by Doyle [5], it can be used for a step towards complete explanation of the crack propagation process in glassy amorphous polymers.

The mean width of the striations in PS decreased strongly in the temperature range 20 to −196° C. In PMMA the differences in band width are dependent principally on molecular weight. There is only a slight increase in band width with increasing temperatures (−196 to 77° C), and no essential influence of the extension rate on the band width was observed.

At higher magnifications in the SEM, all bands

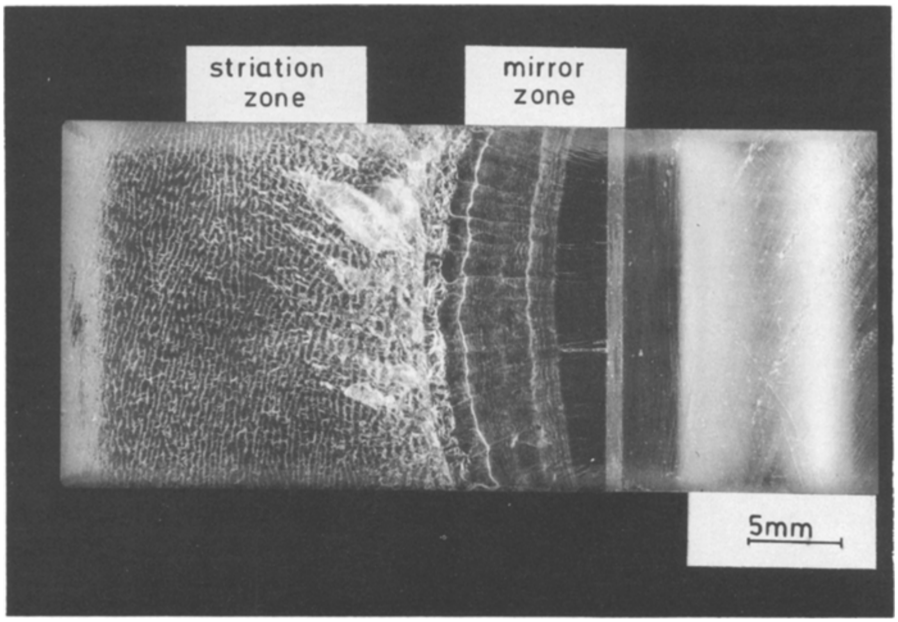

Figure 1 Complete fracture surface of a compact tension specimen of glassy polystyrene produced at room temperature under cyclic loading (mirror region) until fracture occurred by unstable crack propagation (striation zone).